Electronic Supporting Information

A new proton-conducting Bi-carboxylate framework

Sérgio M. F. Vilela, [a] Thomas Devic, [b] Alejandro Várez, [c]

Fabrice Salles, [d] and Patricia Horcajada *[a]

[a] Advanced Porous Materials Unit (APMU), IMDEA Energy Institute, Avda. Ramón de la Sagra 3, E-28935 Móstoles, Madrid, Spain.

[b] Institut des Matériaux Jean Rouxel (IMN) CNRS UMR 6502, Université de Nantes, 2 Rue de la Houssinière, Nantes Cedex 3, France.

[c] Department of Materials Science and Engineering and Chemical Engineering, Universidad Carlos III de Madrid, Avda. Universidad 30, E-28911 Leganés, Madrid, Spain.

[d] Institut Charles Gerhardt de Montpellier (ICGM) UMR 5253 CNRS UM2, Université de Montpellier 2, Place E. Bataillon, 34095 Montpellier Cedex 05, France.

* Correspondence: patricia.horcajada@imdea.org; Tel.: +34 917 371 120

Experimental Section

Reagents and Solvents

Chemicals were readily available from commercial sources and used as received without further purification: 5-nitroisophtalic acid ($C_8H_5O_6N$, 98%, Sigma Aldrich); sodium hydroxide (NaOH, AGR, Labkem); glucose ($C_6H_{12}O_6$, 96%, Sigma Aldrich); hydrochloric acid (HCl, 37%, J.T. Baker); $Bi(NO_3)_3{\cdot}5H_2O$ (98%, Alfa Aesar); potassium acetate (CH_3COOK, extra pure, Merck); *N,N*-dimethylformamide (DMF, p.a., Chem-Lab).

Synthesis

3,3',5,5'-azobenzenetetracarboxylic acid (H_4AzoBTC)

H_4AzoBTC was synthesized according to the procedure reported by Miller *et al.*[1] with slight modifications. Briefly, 5-nitroisophtalic acid (19 g, 20 mmol) was added to a previously prepared solution composed of NaOH (50 g, 1250 mol) and 250 mL of distilled water. The orange mixture was heated at 60 ºC for 30 min under constant magnetic stirring. To the resulting yellowish/brownish mixture, was added a solution composed of glucose (100 g, 555 mmol) already dissolved in 150 mL of distilled water (*note*: if necessary, this mixture should be heated for the complete dissolution of glucose). Then, the obtained mixture was kept at 60 ºC for 15 min, under constant magnetic stirring. After cooling down to room temperature, it was allowed a constant air flow, which was bubbled overnight, under constant magnetic stirring. The resulting brown solid was filtered, transferred for a glass beaker and partially dissolved in 300 mL of distilled water. HCl 37% was added to adjust the pH at 1, leading to the formation of an orange solid, which was filtered and dried in an oven at 70 ºC for 24 h. Yield: 90%wt.

IEF-2 as *Large single-crystals*

A reactive mixture composed of $Bi(NO_3)_3{\cdot}5H_2O$ (0.1820 g, 0.375 mmol) and H_4AzoBTC (0.1343 g, 0.375 mmol), with a molar ratio of 1 : 1 (Bi^{3+} : H_4AzoBTC), 15 mL of distilled water, 50 µL of an aqueous solution of KOH (6 M) and CH_3COOK (0.074 g, 0.754 mmol) was prepared in a 23 mL Teflon-lined autoclave reactor and stirred at room temperature for few minutes. The resulting reaction mixture was placed inside a UN 30^{plus} Memmert convection oven, following the next temperature program: i) heated from room temperature to 120 ºC with a 0.035 ºC min^{-1} rate; ii) kept at 120 ºC for 120 h; and iii) cooled-down to 30 ºC with a 0.031 ºC min^{-1} rate. Suitable single crystals were selected within the mother liquor and placed immediately at 200 K on a single crystal diffractometer (see below), affording $[Bi_4(OH)_2(HAzoBTC)_2(AzoBTC)(H_2O)_4]{\cdot}7H_2O$ (IEF-2).

Scale-up of IEF-2

The synthetic procedure toward the scale-up of IEF-2 was quite similar than that aforementioned. The differences reside in the: i) initial amount of the reagents and solvents (1.401 g of H_4AzoBTC, 1.899 g of $Bi(NO_3)_3{\cdot}5H_2O$, 78 mL of distilled water and 250 µL of an aqueous solution of KOH (6 M)); ii) CH_3COOK was not added; iii) use of a 120 mL Teflon-lined autoclave reactor instead a 23 mL one; and iv) temperature program (heating ramp from room temperature to 120 ºC with a 0.14 ºC min^{-1} rate, kept at 120 ºC for 48 h and cooling ramp to 30 ºC with a 0.13 ºC min^{-1} rate). Recovery, washing and drying processes were the same. IEF-2 was afforded in 86% reaction yield (calculated based on the ligand).

Elemental analyses. Calcd (%) for IEF-2: C 27.03; H 2.08; N 3.94. Found: C 26.16; H 2.44; N 3.49.

Thermogravimetric analysis (TGA) data (weight losses in %) and derivative thermogravimetric peaks (DTG; in italics inside the parentheses): 30-230 ºC –6.91% (*120 ºC*); 230-430 ºC –38.3% (*381 ºC*).

Selected FTIR data (cm^{-1}): $\nu(H_2O)$cryst + $\nu(H_2O)$coord + ν(–OH)coord + ν(–COO-H) = 3600-2700(*br*), ν(=C-H)arom = 3069(*m*), ν(C=O) = 1683(*m*), $\nu_{asym}(-CO_2^-)$ = 1601(*s*), $\nu_{asym}(-CO_2)_{bident}$ = 1524(*s*), ν_{sym}(–N=N–) = 1443(*s*); $\nu_{sym}(-CO_2)_{bident}$ = 1356(*vs*).

General Instrumentation

Powder X-ray diffraction (PXRD) patterns of IEF-2 were collected from 3 to 30° (2θ) using a step size of 0.02° and 2.5 s per step in continuous mode in an Empyream PANALYTICAL diffractometer, equipped with a PIXcel3D detector and with a copper radiation source (Cu Kα, λ =1.5406 Å), operating at 45 kV and 40 mA.

Scanning electron microscopy (SEM) images were collected on a Hitachi TM-100 microscope operating at 15 kV.

Thermogravimetric analyses (TGA) were carried out using a SDT Q-600 thermobalance (TA instruments) under air flow (100 $mL \cdot min^{-1}$) with a heating rate of 5 $^0C \cdot min^{-1}$ between room temperature and 600 °C.

Fourier transform infrared (FTIR) spectra were collected using a Nicolet 6700 instrument with an attenuated total reflectance (ATR) mode by averaging 32 scans at a maximum resolution of 4 cm^{-1} in the 4000-500 cm^{-1} wavenumber range.

^1H and ^{13}C liquid NMR spectra were recorded with a Bruker AVANCE 300 spectrometer at 300.13 and 75.47 MHz, respectively. Deuterated dimethylsulfoxide (DMSO-d_6) was used as solvent.

Single-crystal X-ray diffraction studies

A single crystal of IEF-2 was mounted on a cryo-loop with paratone oil and analyzed at 200(2) K using a Bruker-Nonius Kappa CCD diffractometer working at the Mo Kα radiation. Note here that crystals of IEF-2 desolvate very fast; getting a suitable dataset required attempts on numerous crystals. The Bruker AXS "Collect" suite was used to integrate and scale intensities and a semi-empirical absorption correction (SADABS) were applied on the basis of multiple scans of equivalent reflections. The structure was solved by direct methods, using SHELXS and refined with the full matrix least squares routine SHELXL-2016.[2] Non H-atoms were refined anisotropically. H atoms on the organic fragments were added as rigid bodies, while the one belonging to the water molecules and the hydroxyl bridge were not introduced in the model. After refinement, positive and negative electronic residual densities were found close (*ca.* 1 Å) to the Bi ions. Crystallographic and refinements parameters are summarized in Table S1. CCDC 1908562 contains the supplementary crystallographic data.

Variable-temperature powder X-ray diffraction

Variable-temperature powder X-ray diffraction data for IEF-2 was collected on a X'Pert MPD Philips diffractometer (Cu Kα X-radiation, λ=1.54060 Å), equipped with a X'Celerator detector, a curved graphite-monochromated radiation, a flat-plate sample holder in a Bragg-Brentano para-focusing optics configuration (40 kV, 50 mA), and a high-temperature Antoon Parr HKL 16 chamber controlled by a Antoon Parr 100 TCU unit.

Intensity data for IEF-2 were collected in the step mode (0.03º 2θ, 1 s *per* step) in the range *ca.* $5 \leq 2\theta^{o} \leq 30$. Data were collected between 30 and 600 ºC in intervals of ranging from 20 to 50 ºC.

Proton conductivity

The proton conductivity (σ) of IEF-2 was investigated by electrochemical impedance spectroscopy (EIS) on a pellet with a diameter and thickness of 6.0 and 0.8 mm, respectively. Firstly, the pellet was shaped by uniaxial pressure, applying 6.9 MPa for 5 min and then, isostatically at 4.9 and 19.6 MPa for 10 and 2 min, respectively. Its apparent density was calculated, taking into account their weight and geometric dimensions (*i.e.*, diameter and thickness). Both sides of the pellet were coated by Au ion-blocking electrodes by sputtering in a Leica EM ACE 200 instrument. The electrical measurements were performed on a parallel-plate capacitor configuration in air atmosphere. Measurements were carried out using an Impedance/Gain-Phase Analyzer SI 1260 (Solartron, UK), applying a 100 mV amplitude signal in the in the 10^{-1}-10^{7} Hz frequency range. Measurements at different temperature (RT-80 ºC) and relative humidity (RH) of 80% were performed in a programmable climatic chamber (BINDER, UK). In order to ensure the reproducibility of all measurements, a dwell time of 15 min was defined for the system to reach a stable conditions. By using this method, the RH and temperature could be controlled up to ±1% and ±1 ºC, respectively.

Impedance data analysis was performed using the ZView2 program.[3]

The σ (in S cm^{-1}) is calculated by the following equation:

$$\sigma = \frac{l}{R\ X\ A}$$

where l and A are the thickness (cm) and the area (cm^2) of the pellets, respectively. R is the ohmic resistance (Ohm) obtained from the intersection of the in Nyquist plot of the impedance curve with axis of the real component of the impedance.

Theoretical calculations

In complement to the experimental part, a classical geometry optimization was performed with GULP code on the experimental structure of the partially dehydrated IEF-2 solid (*i.e.*, without free water molecules) with all the H atoms initially placed at tabulated distances as a function of the bonded atoms. For that purpose, partial charges (Figure S10) were extracted using the qEq methodology based on electronegativity equalization approach and Universal Force Field (UFF).[4] The so-obtained structure was the starting point for Monte Carlo simulations to study the impact of water adsorption. Calculations in the Grand Canonical ensemble were performed at 300 K to determine the saturation loading in water molecules inside the IEF-2 structure (Figure S11 and 12) and to extract the plausible configurations of water clusters inside the pores (Figure 3 in the manuscript). 10×10^{6} steps for equilibration and 10×10^{6} steps of production were considered. UFF for long-range interactions and partial charges for the framework were combined with TIP4P-2005 force field[5] for water molecules and implemented in the home-made Monte Carlo code. Regarding the Lennard Jones interactions, the Lorentz-Berthelot rules were applied, as well as a cut-off radius equal to 12.5 Å. In addition, Ewald summation for the electrostatic part was handled to increase the convergence for the energy calculations.

PXRD and SEM

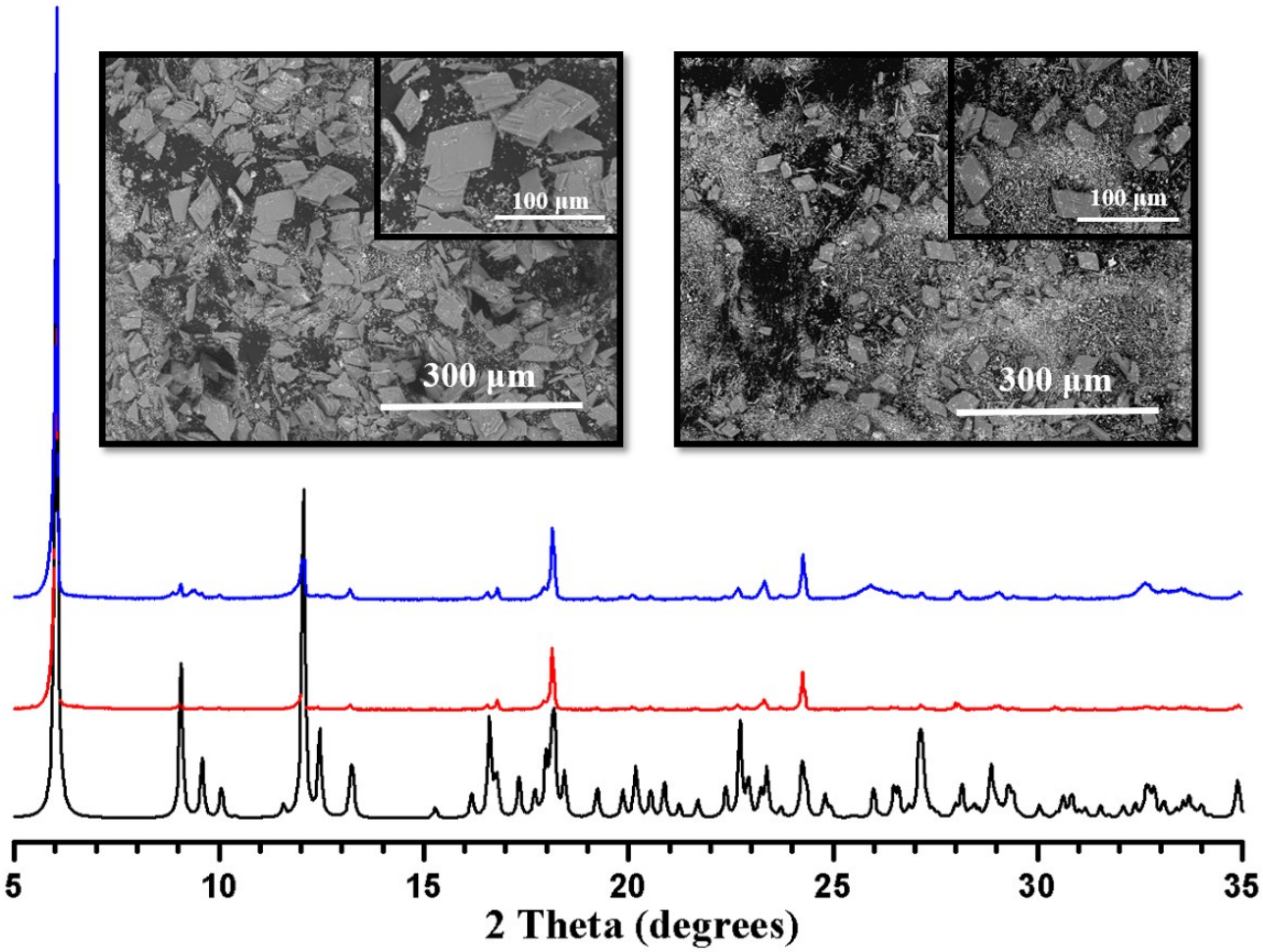

Fig. S1 PXRD patterns of the simulated (black), large single-crystals (**red**) and scale-up (**blue**) IEF-2. Inset: SEM images of IEF-2 isolated as large single-crystals. Note the preferential orientation in red and blue patterns due to the presence of crystalline plate-like morphology.

Crystallographic Studies

Table S1. Crystallographic data and refinement parameters for IEF-2.

Empirical formula	$C_{48}H_{42}Bi_4N_6O_{37}$
Formula weight ($g \cdot mol^{-1}$)	2132.81
Temperature (K)	200(2)
Wavelength (Å)	0.71073
Crystal system	triclinic
Space group	*P*-1
Unit cell dimensions (Å)	a = 9.895(4) b = 10.816(4) c = 15.552(4) α = 97.74(3)° β = 103.42(4)° γ = 111.69(3)°
Volume ($Å^3$)	1459.0(10)
Z, calculated density ($g \cdot cm^3$)	1, 2.427
Adsorption coefficient (mm^{-1})	12.139
F(000)	1002
Crystal size (mm^3)	0.04 x 0.04 x 0.05
Theta range for data collection	2.09° - 29.999°
Limiting indices	$-13 \leq h \leq 13$ $-15 \leq k \leq 15$ $-21 \leq l \leq 21$
Reflections collected / unique	54943/8491 [R(int) = 0.1111]
Refinement method	
Data / Restraints / Parameters	8491/0/428
Goodness of fit on F^2	1.037
Final R indices [I > 2σ(I)]	R1 = 0.0602 wR2 = 0.1257
R indices (all data)	R1 = 0.1270 wR2 = 0.1548
Largest diff peak and hole ($e \cdot Å^{-3}$)	2.923 and -2.418

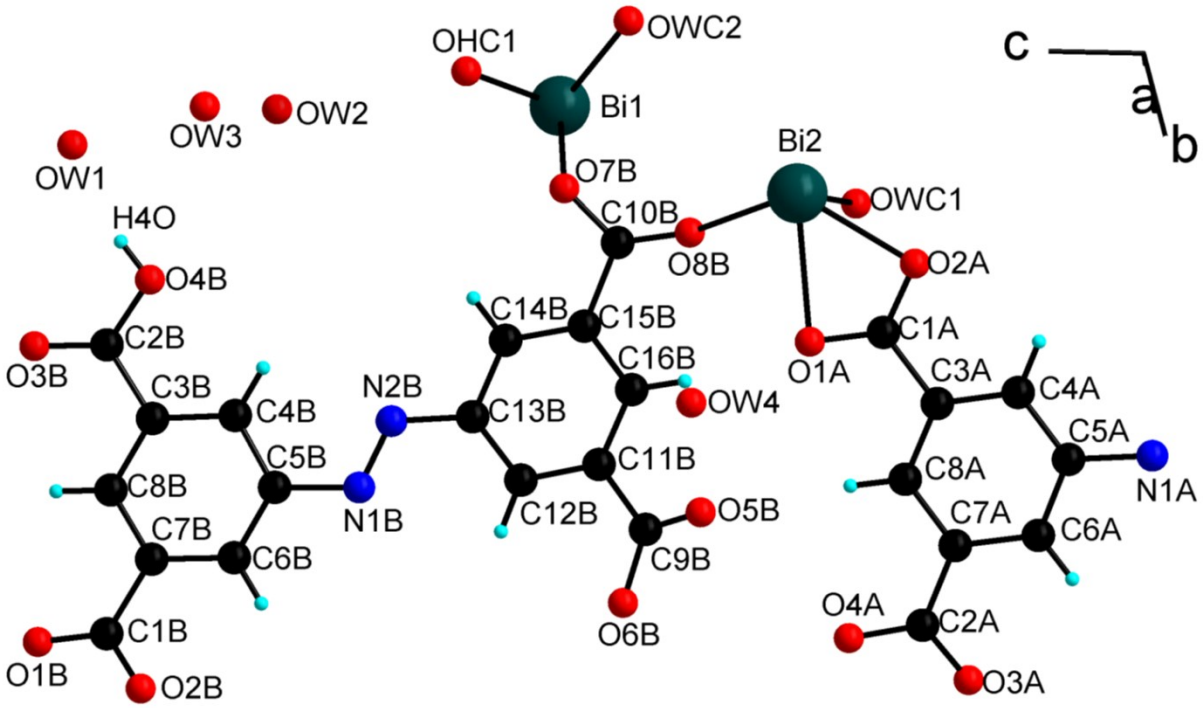

Fig. S2 Representation of the asymmetric unit of IEF-2.

Table S2. Bond valence calculations.[6]

Atomic pair	*Distance (Å)*	*Valence*
Bi-1OHC1	2.129(8)	0.90
Bi1-O3A	2.364(8)	0.48
Bi1-O7B	2.379(8)	0.46
Bi1-O6B	2.392(8)	0.44
Bi1-O5B	2.554(9)	0.29
Bi1-OWC2	2.652(9)	0.22
Bi1-O4A	2.691(9)	0.20
Bi1-O4A	2.729(8)	0.18
	total Bi1	**3.16**
Bi2-O2B	2.282(8)	0.59
Bi2-O2A	2.313(8)	0.55
Bi2-OHC1	2.316(8)	0.54
Bi2-OWC1	2.411(9)	0.42
Bi2-O1A	2.508(9)	0.32
Bi2-O8B	2.633(9)	0.23
Bi2-O1B	2.705(8)	0.19
Bi2-O7B	2.798(11)	0.15
	total Bi1	**2.99**
OHC1-Bi1	2.129(8)	0.90
OHC1-Bi2	2.316(8)	0.54
	total OHC1	**1.44**

Table S3. Hydrogen bonds: short donor-acceptor distances.

Donor	*Acceptor*		*Distance*
O4B	OW1	1-x, 1-y, 1-z	2.649
OHC1	O3B	1-x, 2-y, 1-z	2.680
OW4	O1A	-x, 3-y, -z	2.939
OW1	O3A	1-x, 2-y, -z	2.927
OWC1	O6B	1-x, 3-y, -z	2.743
OWC2	O1B	-1+x, -1+y, -1+z	2.838
OW4	O5B	-x, 3-y, -z	2.710
OW4	O5B	x, y, z	2.730
OW2	OWC1	1-x, 2-y, -z	2.726
OW2	OW3	1-x, 2-y, 1-z	2.729
OW4	OWC2	-x, 2-y, -z	2.695

FTIR Spectroscopy

FTIR shows the symmetric and asymmetric –CO stretching vibration modes (at the *ca.* 1420-1345 and 1580-1515 cm^{-1} spectral ranges, respectively), representative of bidentate and bridging carboxylates (*i.e.*, identified by the crystallographic O1-O2 and O7-O8 atoms, respectively; see Figure S2 in the ESI),[7] supporting the coordination of the bismuth ion to the carboxylate ligand. The asymmetric stretching vibration of the deprotonated $–CO_2^-$ and the symmetric one, attributed to the azo compounds (*i.e.*, –N=N–) are also assigned at *ca.* 1601 and 1443 cm^{-1} (the later appears at *ca.* 1456 cm^{-1} for the solely H_4AzoBTC), respectively. The spectrum of IEF-2 between 3600 and 2700 cm^{-1} is dominated for some broad bands related with the presence of the characteristic –O-H and –C-H stretching vibrations, which are attributed to the free carboxylic acid groups, water of crystallization and coordinated water molecules and hydroxyl moieties. In this line, the –C=O stretching vibration mode is centered at *ca.* 1683 cm^{-1}, corresponding to the non-coordinated carboxylic acid functional groups presented in IEF-2, corroborating the crystallographic analysis. Note that, the same band, centered at *ca.* 1686 cm^{-1}, is also identified in the spectrum of the free organic molecule, but quite stronger due to the presence of four carboxylic acids in H_4AzoBTC.

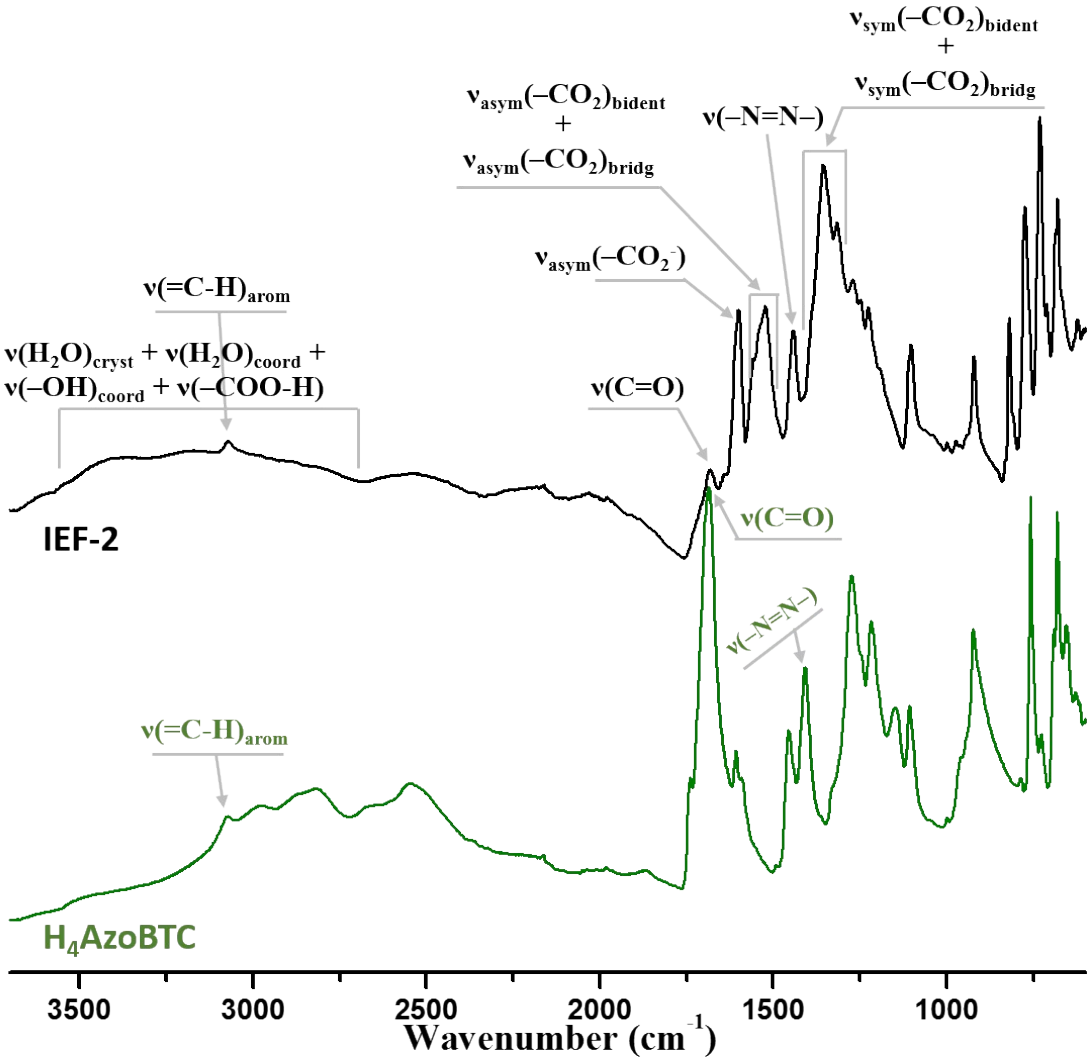

Fig. S3 FT-IR spectra of IEF-2 (**black**) and the organic linker H_4AzoBTC (**green**).

Thermal and Chemical Stability

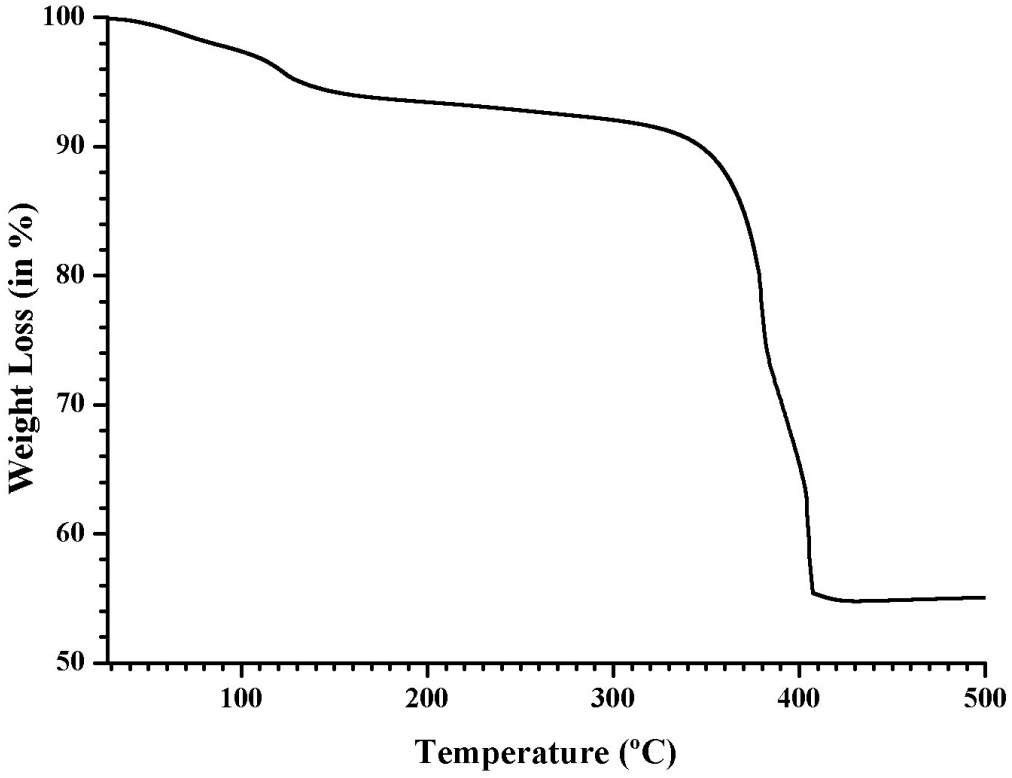

Fig. S4 TGA of IEF-2.

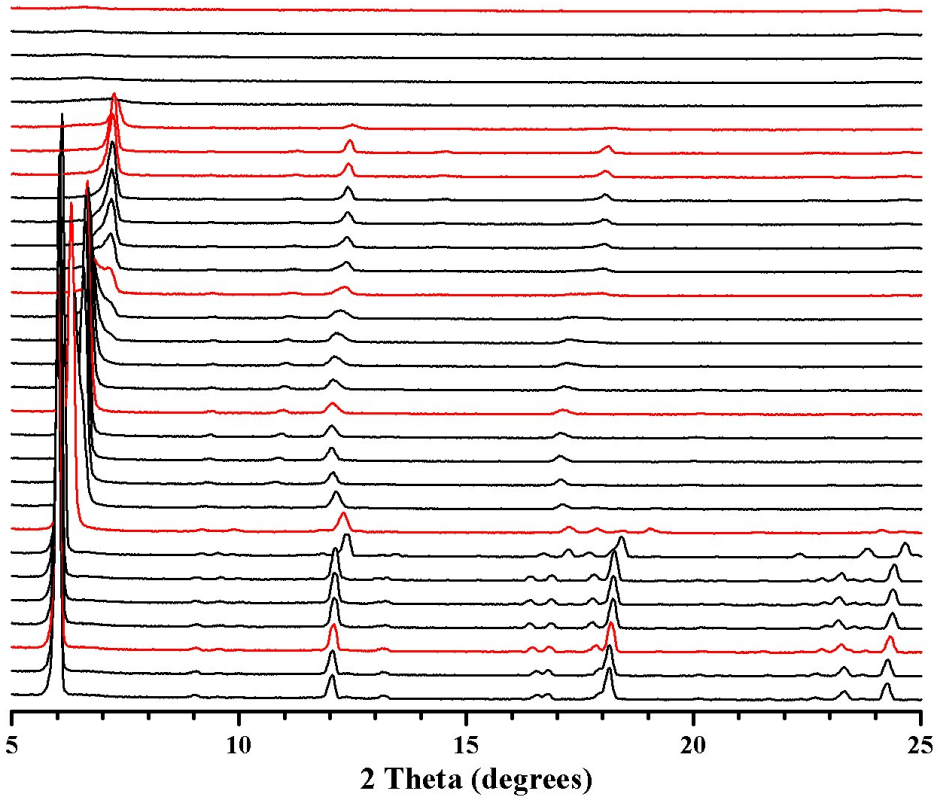

Fig. S5 Temperature dependent XRD patterns of IEF-2 from 30 to 400 ºC. Each **red** line corresponds an increment of 50 ºC.

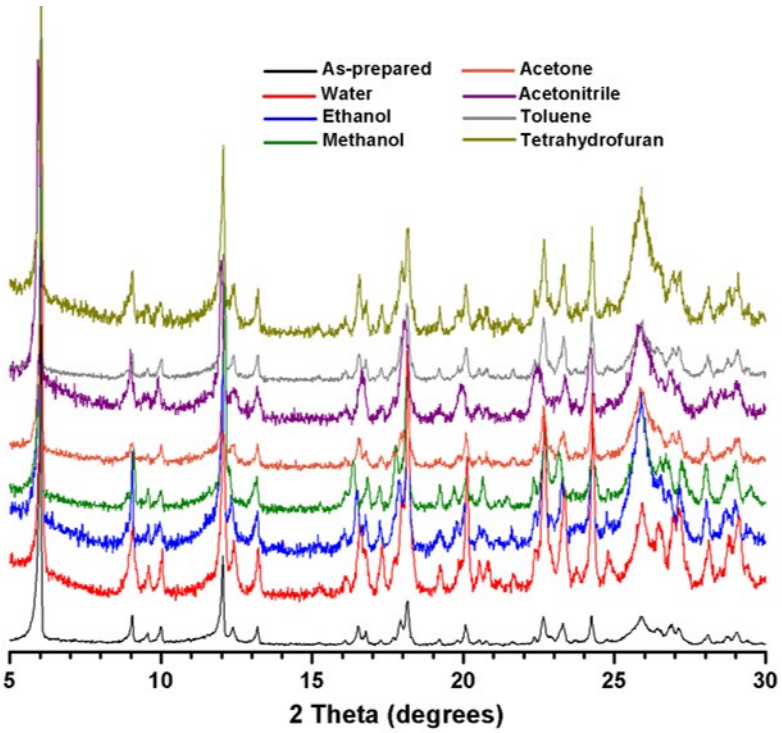

Fig. S6 PXRD patterns of the as-prepared IEF-2 and after its suspension in different solvents for 6 days at room temperature.

Proton Conductivity

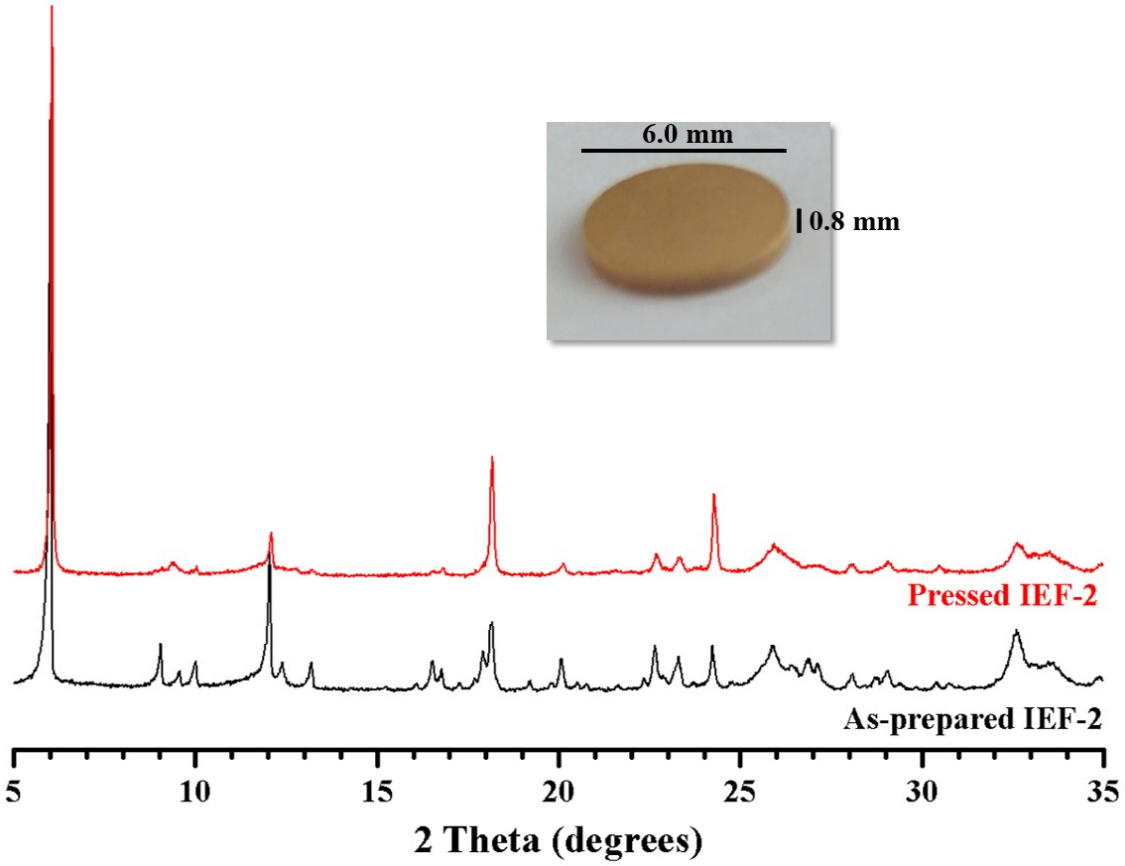

Fig. S7 PXRD of the as-prepared IEF-2 (**black**) and after press-molding at 20 MPa (**red**). Inset: photography of IEF-2 as a disk-like pellet pressed at 20 MPa with its diameter and thickness dimensions. IEF-2 maintains its structural integrity as well as its overall crystallinity after the used pressing protocol.

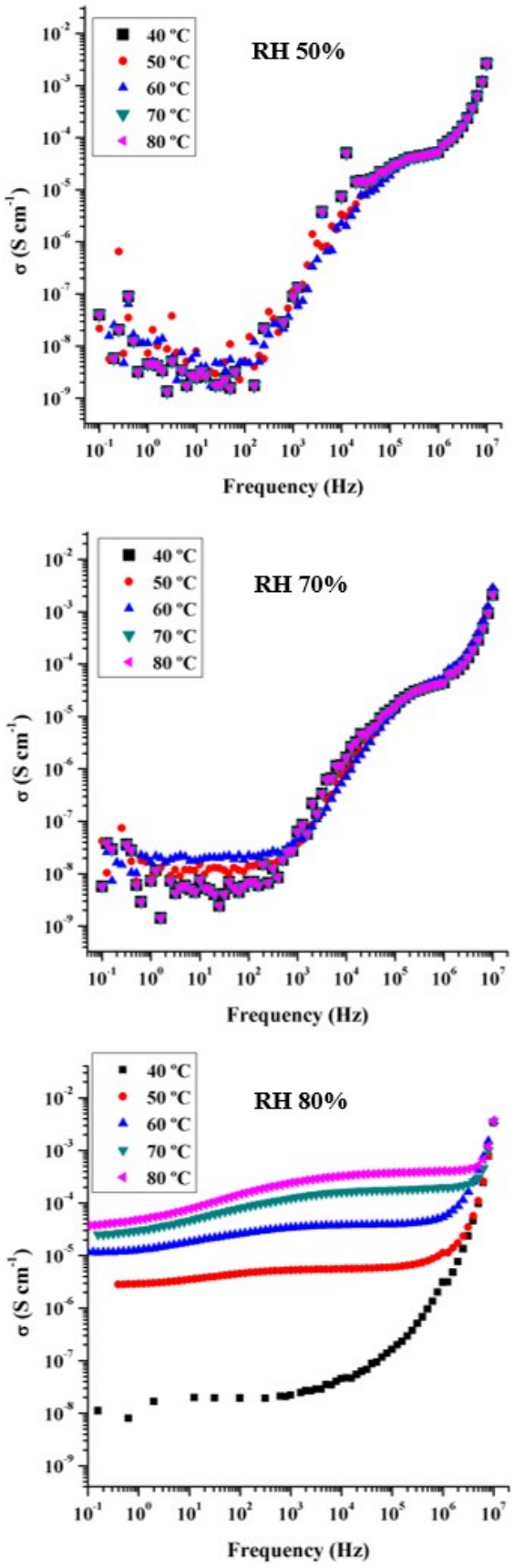

Fig. S8 Evolution of the conductivity with the frequency of IEF-2 at RH 50, 70 and 80%. A large dispersion in the low frequency region is displayed with very high impedance values ranged between 10^{-7} and 10^{-9} S cm^{-1} within the instrumental precision.

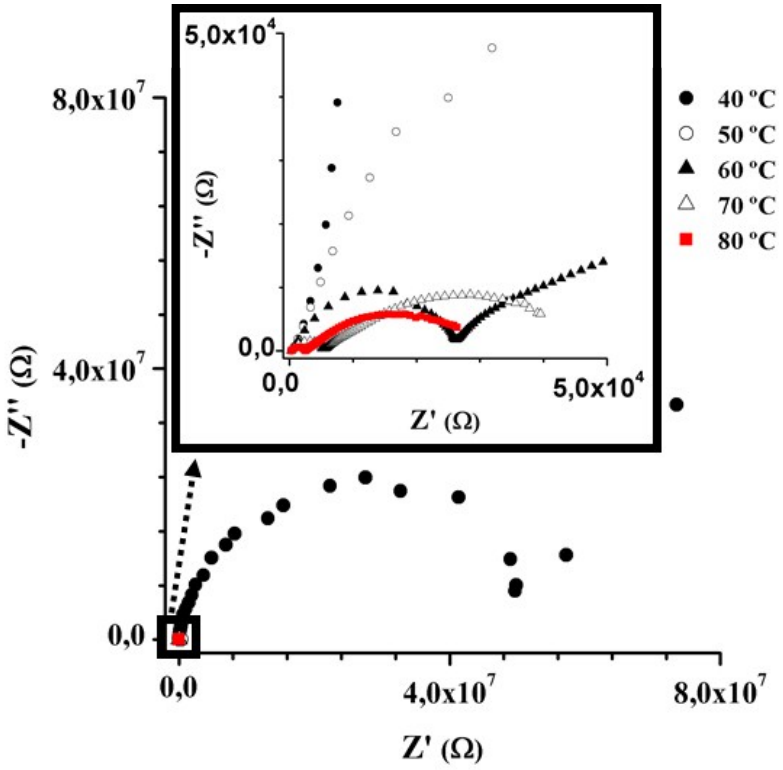

Fig. S9 Nyquist plots for IEF-2 collected at 80% RH and different temperatures.

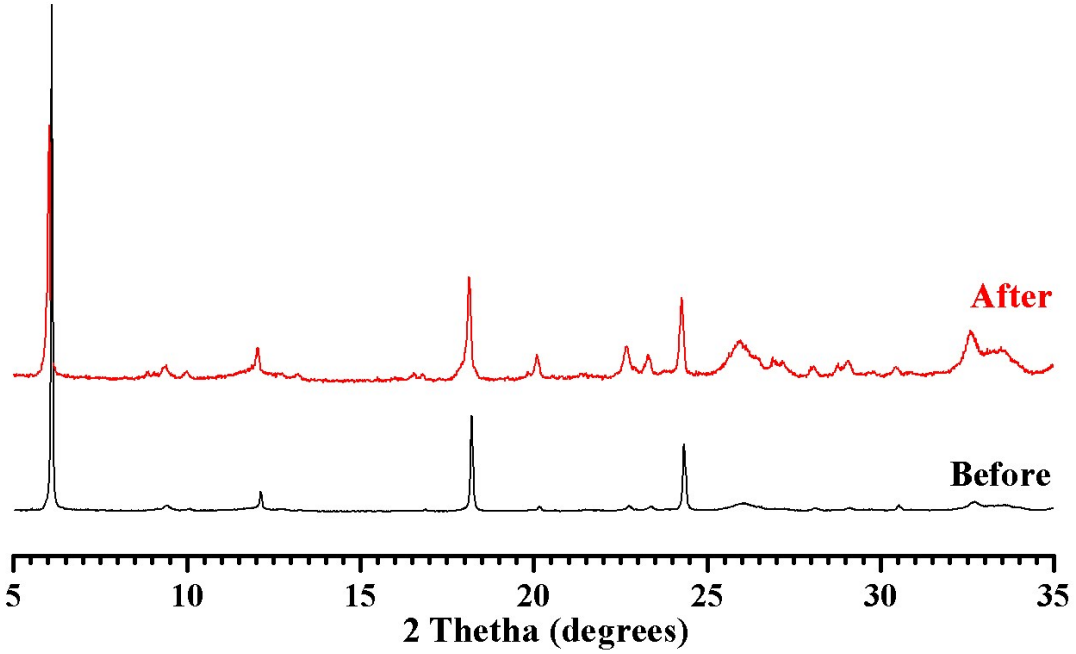

Fig. S10 PXRD of the pressed IEF-2 before (**black**) and after (**red**) proton conductivity measurements. Besides some loss of crystallinity, any significant structural change is noticed.

Theoretical Calculations

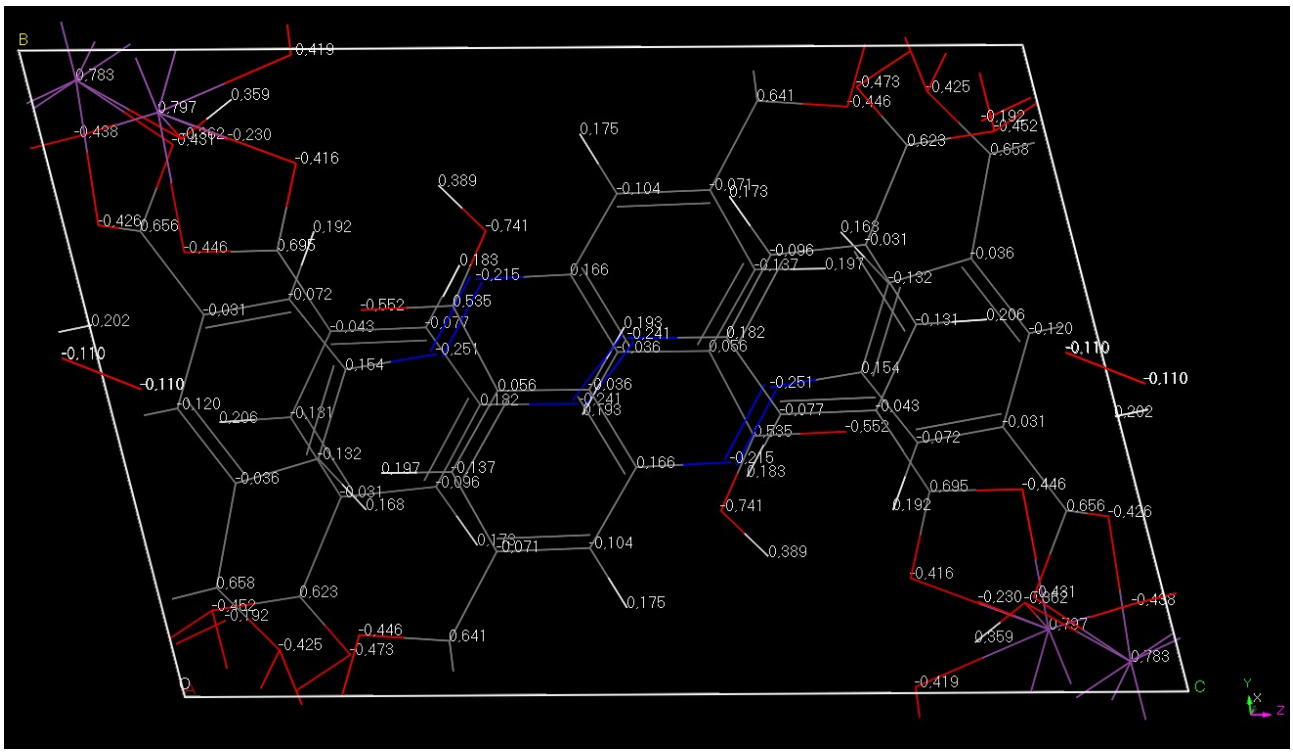

Fig. S11 Schematic representation of the partial charges calculated for IEF-2.

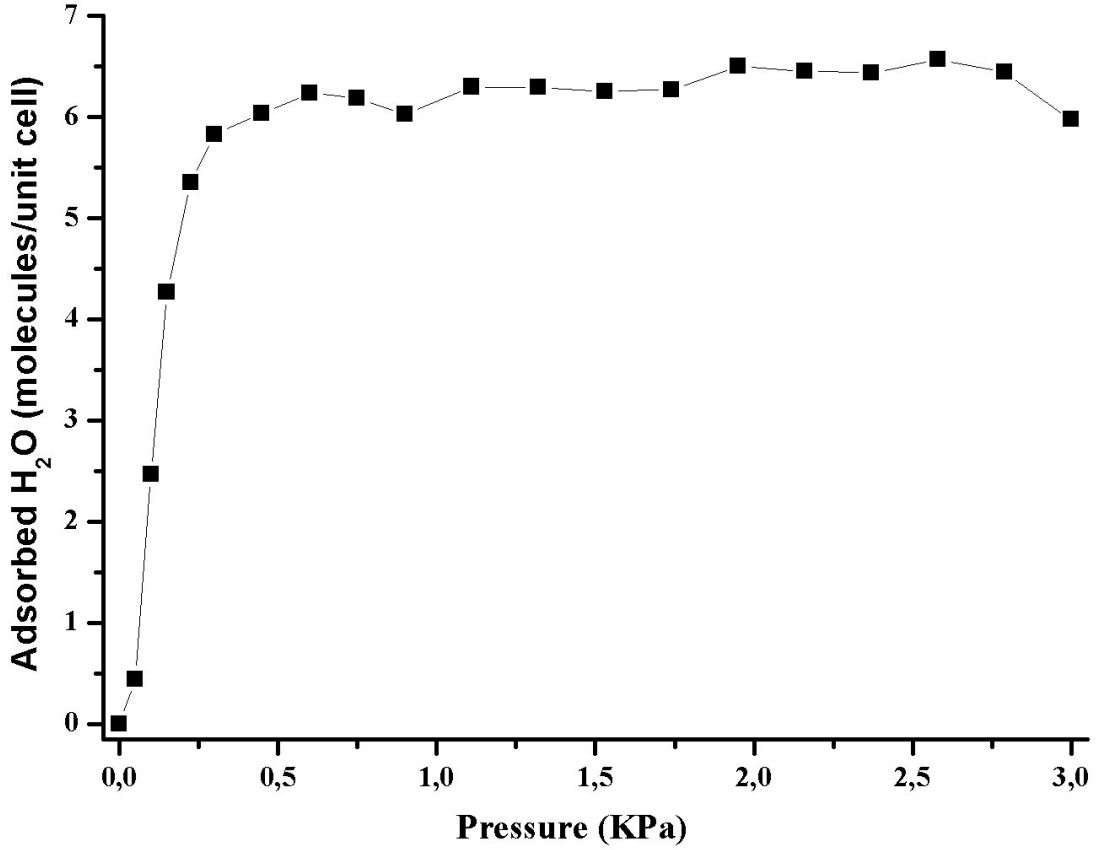

Fig. S12 Water adsorption isotherm estimated at 300 K for IEF-2 by GCMC simulations.

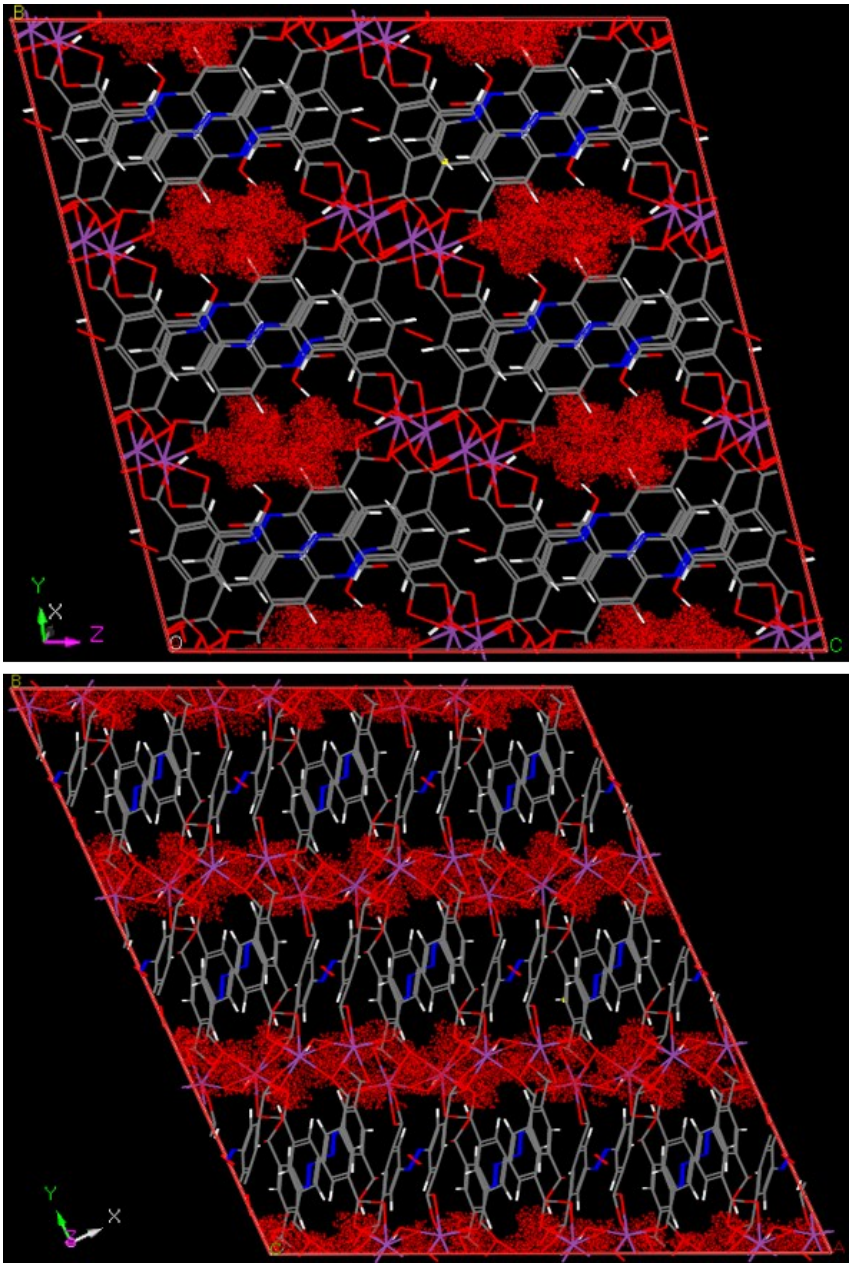

Fig. S13 Snapshots representing the density probability for the presence of water molecules in the pores, according to the (yz) and (xy) directions, illustrating also the distribution of such molecules in IEF-2 at water saturation and ambient temperature. Red spots correspond to probable sites where water molecules are located. Color code: C = **grey**, H = , O = **red**; N = **blue** and Bi = **purple**.

References

1 S. R. Miller, E. Alvarez, L. Fradcourt, T. Devic, S. Wuttke, P. S. Wheatley, N. Steunou, C. Bonhomme, C. Gervais, D. Laurencin, R. E. Morris, A. Vimont, M. Daturi, P. Horcajada and C. Serre, *Chem. Commun.*, 2013, **49**, 7773–7775.

2 G. M. Sheldrick, *Acta Crystallogr. Sect. A*, 2015, **71**, 3–8.

3 Zview 2 for Windows (Version 2.0). Scribner Assoc. Inc., Charlottesville, VA, USA (2000).

4 A. K. Rappé, C. J. Casewit, K. S. Colwell, W. A. Goddard and W. M. Skiff, *J. Am. Chem. Soc.*, 1992, **114**, 10024–10035.

5 J. L. F. Abascal and C. Vega, *J. Phys. Chem.*, 2005, **123**, 234505.

6 M. O'Keefe and N. E. Brese, *Acta Cryst.*, 1991, **B47**, 192–197.

7 G. Socrates, *Infrared Characteristic Group Frequencies*, John Wiley & Sons, Chichester, 2nd edn., 1994.